Electronic Supplementary Material (ESI) for ChemComm.
This journal is © The Royal Society of Chemistry 2019

Supporting information for

Anchoring Carbon Nanotubes and Post-Hydroxylation Treatment Enhanced Ni Nanofiber Catalysts towards Efficient Hydrous Hydrazine Decomposition for an Effective Hydrogen Generation

Experimental Section

Materials. Nickel acetate tetrahydrate ($NiAc{\cdot}4H_2O$), polyvinylpolypyrrolidone (PVP, M_w = 1, 300, 000), acetic acid (HAc), ethanol (EtOH), hydrous hydrazine ($N_2H_4{\cdot}H_2O$, 85%), hydrochloric acid (HCl) and sodium hydroxide (NaOH) were obtained from Aladdin Ltd. (Shanghai, China). All chemicals were used as received without any purification.

Preparation of Ni-CNTs. A typical precursor solution was prepared by mixing 1.4 g $NiAc{\cdot}4H_2O$, 0.5 g PVP, 1.5 mL HAc in 12 mL EtOH with vigorous stirring until a homogeneous and viscous solution was formed. The obtained solution was transferred into a plastic syringe (10 mL) with a capillary tip of 0.6 mm diameter. The voltage of 60 kV was applied with a distance of 15 cm. A film of NiAc/PVP composite nanofibers was electrospun on a piece of aluminum foil. NiAc/PVP composite nanofibers were placed into a quartz crucible and then calcined in a quartz pipe furnace at 773 K for 3 h with 1 K min^{-1} heating rate under vacuum condition to obtain Ni nanofiber (Ni-NF). After quartz pipe furnace was cooled down to room temperature, Ni-CNTs were synthesized via a following vacuum chemical vapor deposition (CVD) method. A certain amount of PVP as solid carbon source, was introduced into another quartz crucible. After 773 K treatment for 3 h under vacuum condition, Ni-CNTs nanofibers were obtained.

Hydroxyl Functionalization of Ni-CNTs (*Ni-CNTs-OH)*. The Ni-CNTs-OH were prepared by a typical hydroxylation procedure. Briefly, the obtained Ni-CNTs (0.1 g) were mixed with 1.0 g KOH in 20 mL ethanol. The solution was gently stirred at 323 K for 12 h. After the hydroxylation procedure was finished, the suspension was washed by deionized water until the pH value reached 7, and then dried at 333 K under vacuum for 24 h.

Catalyst characterization. The morphologies of Ni, Ni-CNTs and Ni-CNTs-OH nanofibers were characterized using a high-resolution scanning electron microscopy (SEM, Hitachi S4800) and transmission electron microscopy (TEM, Hitachi HT7700). The crystal structures and compositions of the Ni-CNTs nanofibers were measured by X-ray diffraction (XRD, Bruker D8) with Cu-K_α radiation (λ = 0.15418 nm) at 40 kV and 40 mA. The scanning angle (2θ) range was varied from 10^o to 90^o, operated at a scan speed of 10 min^{-1}. Before test, all

samples were vacuum degassed for 12 h at a pressure less than ~ 10^{-7} Pa. The N_2 adsorption-desorption isotherms were collected on a surface area analyzer (Quantachrome NOVA 4000e) at 77 K. Before adsorption, all samples were dried at room temperature and then degassed under vacuum at 573 K for 5 h. The pore size distributions were collected by the Barrett-Joyner-Halenda (BJH) model using the desorption branch of the isotherm. Water contact angles (CA) measurements were performed on an optical contact angle measuring apparatus (XG-CAMA1). Before measurement, all the samples were pressed into flakes under a pressure of 5 MPa. Fourier transform infrared (FT-IR, Nicolet 5700) spectra were used to characterize the oxygen-containing groups on the surface of the synthesized CNTs.

Catalytic test. In a typical experiment, a specific amount of Ni-CNTs or Ni-CNTs-OH catalysts were dispersed in NaOH solution (1.0 M, 3 mL) with magnetic stirring for 10 min at a constant temperature, and then a calculated amount of hydrous hydrazine was added into the suspension. To ensure that the evolved gases measured on the gas burette only contain H_2 and N_2, the by-product NH_3 was absorbed by HCl solution (1.0 M) before measured volumetrically. The long-term durability of the as-synthesized catalysts was carried out. Ten cycles of reactions were taken over the same catalyst at 333 K with 1.0 M NaOH solution, after the first cycle of hydrous hydrazine decomposition reaction was completed, another equivalent of hydrous hydrazine was introduced into reactor vessel.

The selectivity of H_2 generation from hydrous hydrazine (defined as X) was evaluated by $X = \frac{3Y-1}{8}, (Y = \frac{n_{(N2+H2)}}{n_{N2H4}}, \frac{1}{3} \leq Y \leq 3)$, which could be derived based on $N_2H_4 \rightarrow N_2 + 2H_2$ and $3N_2H_4 \rightarrow 4NH_3 + N_2$. The turnover frequencies (TOFs) of all catalysts for the decomposition of hydrous hydrazine were defined as the number of converted hydrazine in per metal Ni atom per hour when the conversion of hydrazine reached 50%.

Results and Discussion

The morphologies of Ni-NF, Ni-CNTs and Ni-CNTs-OH are shown in Fig. S1. It can be seen that the prepared Ni-NF exhibit smooth and uniform fibrous structure, with a diameter of ~ 200 nm. Moreover, a cross-linked structure can be also observed. With Ni-NF as catalyst and PVP as solid carbon source, CNTs can grow at 500 ^{o}C in a vacuum condition to form Ni-CNTs, as given in Fig. S1d-f. The obtained CNTs show an entangled and zigzag structure, with an outer diameter of 10-40 nm. Fig. S1h-l shows the SEM and TEM images of Ni-CNTs-OH, which indicate that the Ni-CNTs-OH exhibit similar morphology to Ni-CNTs. Fig. S2 shows the TEM images of the CNTs dropped from the Ni nanofibers. It can been seen that the outer diameter of CNT is around 10 nm and inner diameter is around 1-2 nm.

The crystalline structures of the as-synthesized catalysts were analyzed by XRD (Fig. S3). Three observed distinctive peaks at $2\theta = 44.5^{o}$, 51.8^{o} and 76.4^{o} correspond to the (111), (200), and (220) planes of face-centered cubic (FCC) Ni (JCPDS No. 04-0805), respectively. This result indicates that Ni was formed after a vacuum heat-treatment. Besides hydrogen (H_2), it has been demonstrated that Ni^{2+} could also be reduced by other reductants in thermal treatment process, such as carbon (C) and carbon monoxide (CO). Such kinds of reductants (H_2, C, CO) can be generated from the NiAc/PVP composite nanofibers during the thermal treatment process.

The X-ray photoelectron spectrum (XPS) measurement was further performed to investigate the electronic state of Ni-CNTs and Ni-CNTs-OH (Fig. S4). In the Ni 2p spectrum of Ni-CNTs (Fig. S4b), the peak with a binding energy of 852.9 eV is assigned to Ni $2p_{3/2}$. Two lower intensity peaks at 855.6 and 873.3 eV are assigned to Ni^{2+} $2p_{3/2}$ and $2p_{1/2}$, respectively. The results demonstrate that the major phase of Ni-CNTs nanofibers is metal Ni with a few oxide species on the surface. After hydroxylation modification, the intensity of Ni^{2+} is increased, which indicates that some Ni has been oxidized after hydroxylation modification (Fig. S4d). However, NiO has not been detected by XRD (Fig. S3). It worths to note that no sodium (Na) detected in Ni-CNTs-OH (Fig. S4c) means no adsorption of Na^{+} on Ni-CNTs-OH after NaOH treatment.

Fig. S5 and Fig. S6 are the Raman spectra and FT-IR spectra of Ni-CNTs and Ni-CNTs-OH. Both Ni-CNTs and Ni-CNT-OH show two absorption bands at 1195 and 1540 cm^{-1}, which can be attributed to the stretching

vibration of C-O and C=C, respectively.[1] Compared with Ni-CNTs, the stronger C-O band of Ni-CNTs-OH may arise from the hydroxylation of the sp^2 C atoms on the surface of CNTs. The appearance of a broad absorption band at 3409 cm^{-1} was due to the presence of -OH groups on the surface of the CNTs, suggesting that -OH group was introduced into CNTs successfully through KOH/EtOH treatment.

The contact angles of Ni-CNTs-OH and Ni-CNTs-OH after ten cycles of catalytic degradation are shown in Fig. S7. The contact angle of Ni-CNTs-OH is 48.4^o, which almost remain the same for Ni-CNTs-OH after ten cycles of catalytic degradation (48^o). As shown in Fig. S8, some Ni nanofibers were cracked after first cycle, while their fibroid shapes were still maintained (Fig. S8a). With supporting of CNTs, Ni-CNTs-OH maintain their original shape after first cycle (Fig.S8 b and c). The increases in the specific surface areas of Ni-CNTs compared with the parent Ni-NF suggests that the CNTs have been successfully grown on Ni-NF. After KOH/EtOH treating, the specific surface area and the amount of mesopores slightly increases. Fig. S11 is Na 1s XPS spectrum of Ni-CNTs-OH after ten cycles of catalytic degradation. There is no element of Na detected even after ten cycles of catalytic degradation, which indicates Na^+ will not occupy on active sites of Ni-CNTs-OH.

References

1 P. Liu, X. Gu, Y. Wu, J. Cheng, H. Su, *Int. J. Hydrogen Energ.,* 2017, **42**, 19096.

2 L. He, Y. Huang, A. Wang, X. Wang, X. Chen, J. J. Delgado, T. Zhang, *Angew. Chem., Int. Edit.,* 2012, **51**, 6191.

3 A. K. Singh, M. Yadav, K. Aranishi, Q. Xu, *Int. J. Hydrogen Energ.,* 2012, **37**, 18915.

4 S. K. Singh, A. K. Singh, K. Aranishi, Q. Xu, *J. Am. Chem. Soc.,* 2011, **133**, 19638.

5 S. K. Singh, Q. Xu, *Chem. Commun.,* 2010, **46**, 6545.

6 S. K. Singh, Q. Xu, *J. Am. Chem. Soc.,* 2009, **131**, 18032.

7 W. Kang, A. Varma, *Appl. Catal. B: Environ*., 2018, **220**, 409.

8 X. Chen, H. Wang, S. Gao, Z. Wu, *J. Colloid. Interf. Sci.,* 2012, **377**, 131.

9 D. Wu, M. Wen, X. Lin, Q. Wu, C. Gu, H. Chen, *J. Mater. Chem. A,* 2016, **4**, 6595.

10 H. L. Wang, J. M. Yan, Z. L. Wang, S. Il O, Q. Jiang, *J. Mater. Chem. A,* 2013, **1**, 14957.

11 J. Wang, Y. Li, Y. Zhang, *Adv. Funct. Mater.,* 2014, **24**, 7073.

12 Q. Fu, P. Yang, J. Wang, H. Wang, L. Yang, X. Zhao, *J. Mater. Chem. A,* 2018, **6**, 11370.

13 L. He, Y. Huang, X. Liu, L. Li, A. Wang, X. Wang, C. Mou, T. Zhang, *Appl. Catal. B: Environ*., 2014, **147**, 779.

14 H. Dai, Y. Qiu, H. Dai, P. Wang, *ACS Sustainable Chem. Eng.,* 2018, **6**, 9876.

15 A. Kumar, X. Yang, Q. Xu, *J. Mater. Chem. A*, 2019, **7**, 112.

Table and Figures

Table S1. Comparison summary of reported similar catalysts.

Catalyst	T (K)	TOF (h^{-1})	Selectivity (%)	Reference
Ni/MIL-101-NH_2	298	1.3	-	1
Ni/Al_2O_3	303	2.2	93	2
$Ni_{90}Rh_{10}$	323	3.3	100	3
NiFe	343	4.2	100	4
$Ni_{0.95}Ir_{0.05}$	333	4.4	100	5
Rh_4Ni	298	4.8	100	6
Ni/CeO_2 (6 wt% Ni)	323	5.1	95	7
$Ni_{0.6}Pd_{0.4}$	343	5.5	82	8
NiCo/NiO-CoO_x	298	5.9	99	9
$Ni_{0.9}Pd_{0.1}$	298	6.4	100	10
Cu@Fe_5Ni_5	343	11.9	100	11
Nickel nanofibers	333	6.9	100	12
$NiIr_{0.059}/Al_2O_3$	303	12.4	98	13
Ni-CNTs-OH	**333**	**19.4**	**100**	**This work**
Ni-Pt/CeO_2/GAC	323	-	100	14
$Pt_{0.5}Ni_{0.5}$ /NGNs-850	303	943	100	15

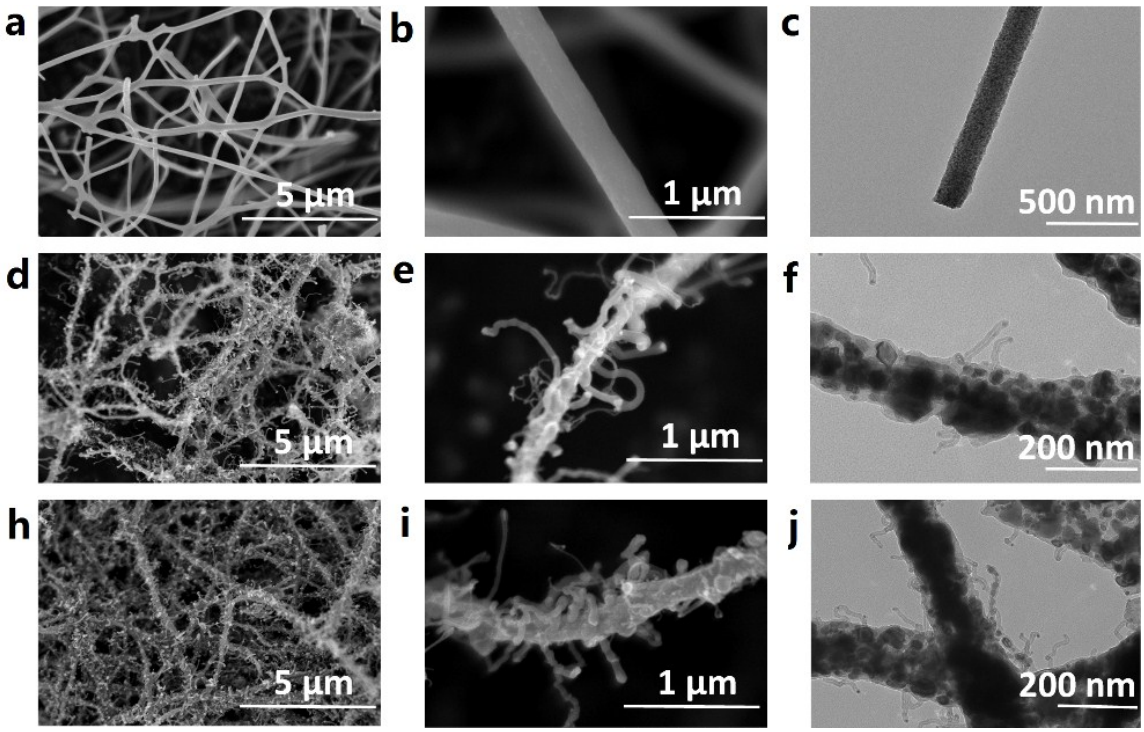

Fig. S1 SEM and TEM images of (a, b, c) Ni-NF, (d, e, f) Ni-CNTs and (h, k, l) Ni-CNTs-OH.

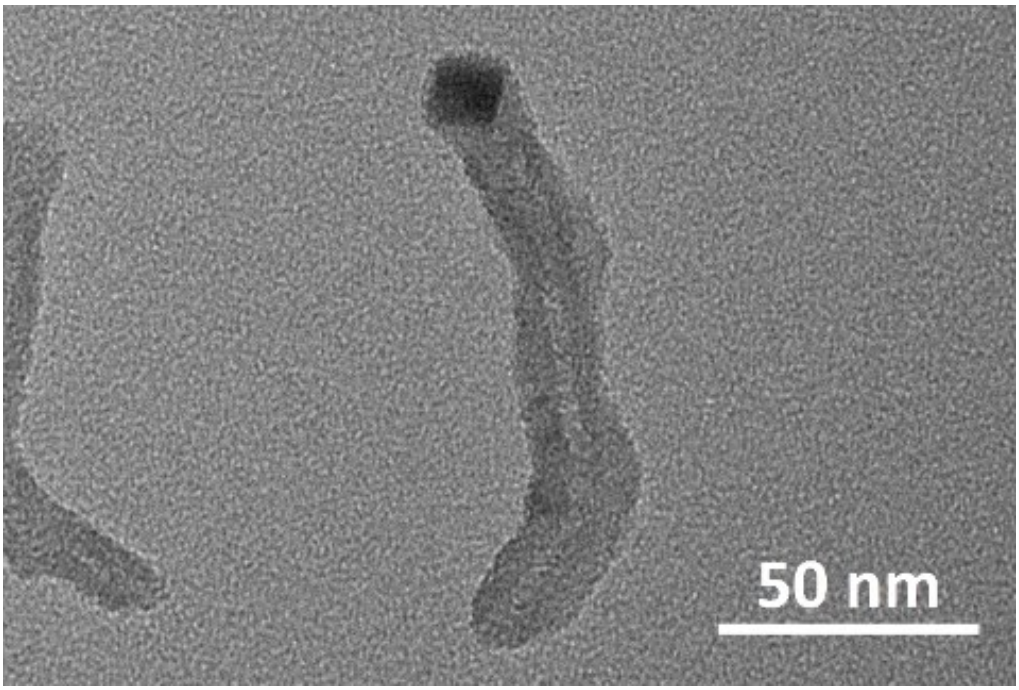

Fig.S2 TEM image of CNTs dropped from Ni nanofibers.

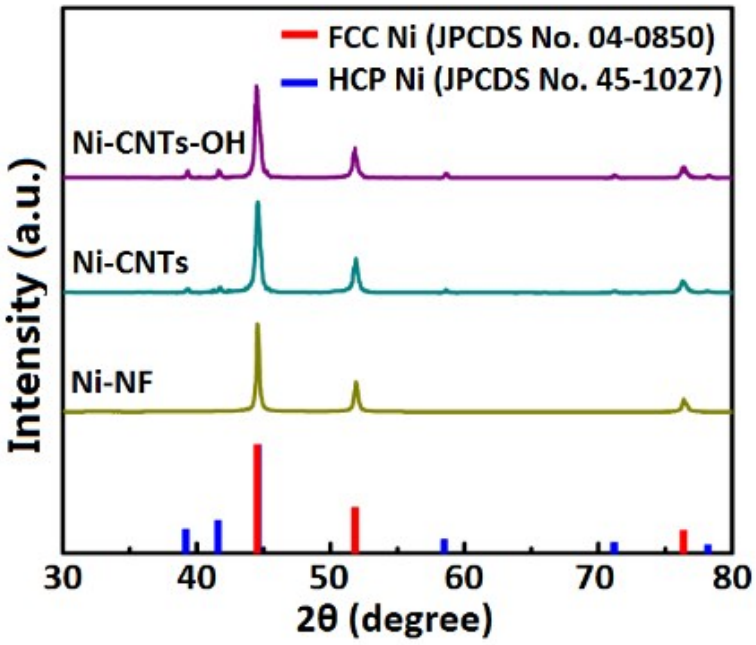

Fig. S3 XRD patterns of the as-synthesized Ni-NF, Ni-CNTs and Ni-CNTs-OH.

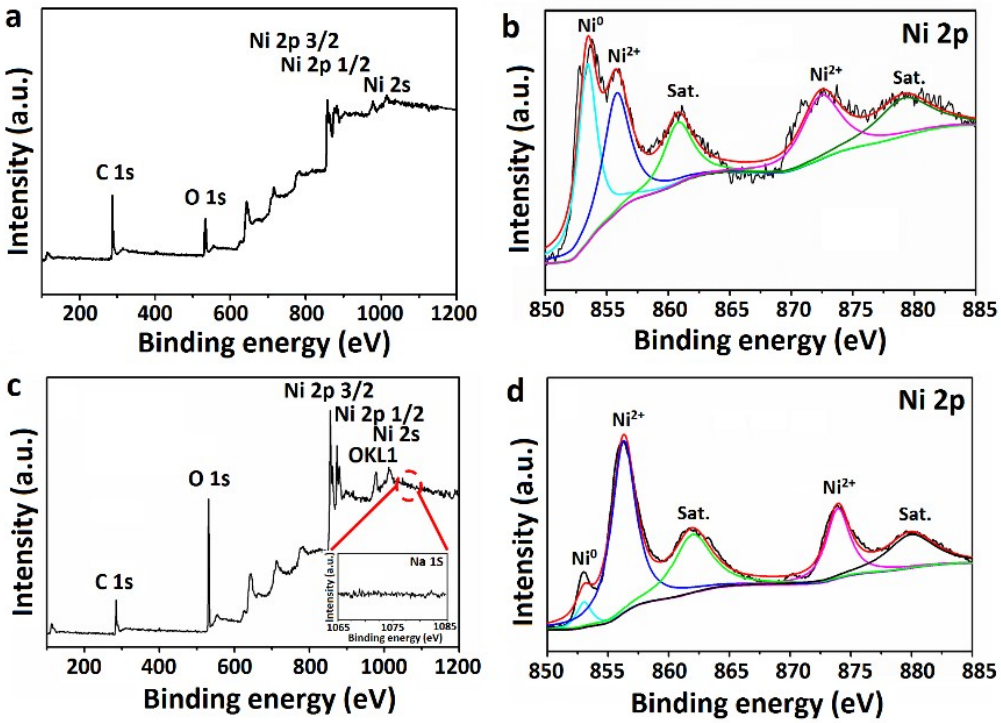

Fig. S4 XPS survey and Ni 2p spectra of (a, b) Ni-CNTs and (c, d) Ni-CNTs-OH.

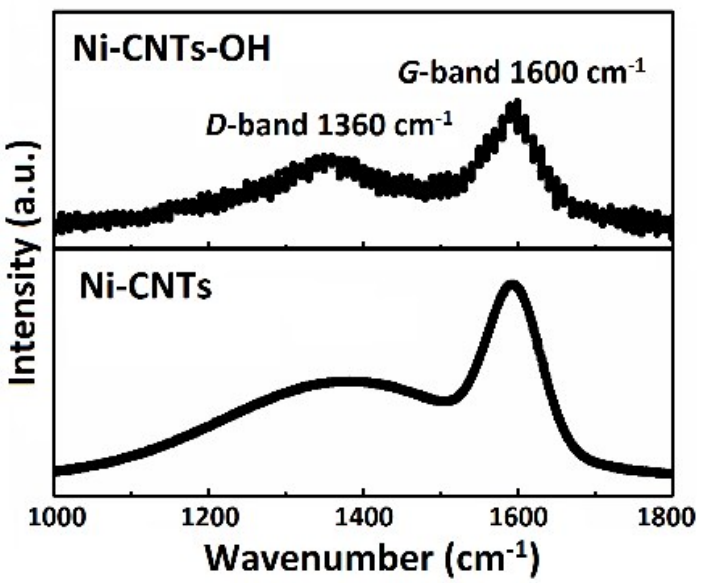

Fig. S5 Raman spectra of Ni-CNTs and Ni-CNTs-OH samples.

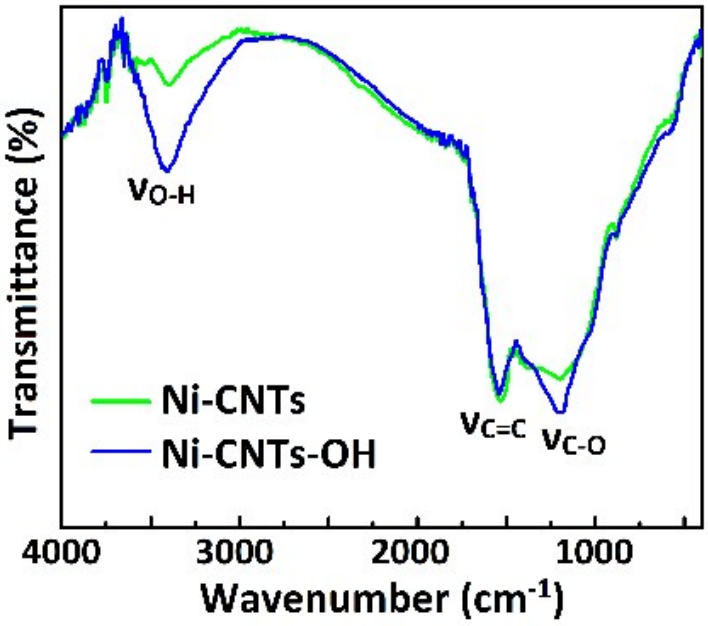

Fig. S6 FT-IR spectra of Ni-CNTs and Ni-CNTs-OH.

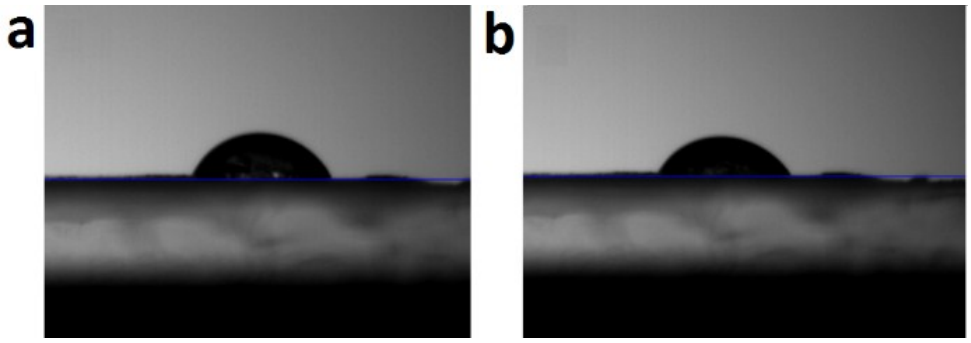

Fig. S7 Contact angles of (a) Ni-CNTs-OH and (b) Ni-CNTs-OH after ten cycles of catalytic degradation.

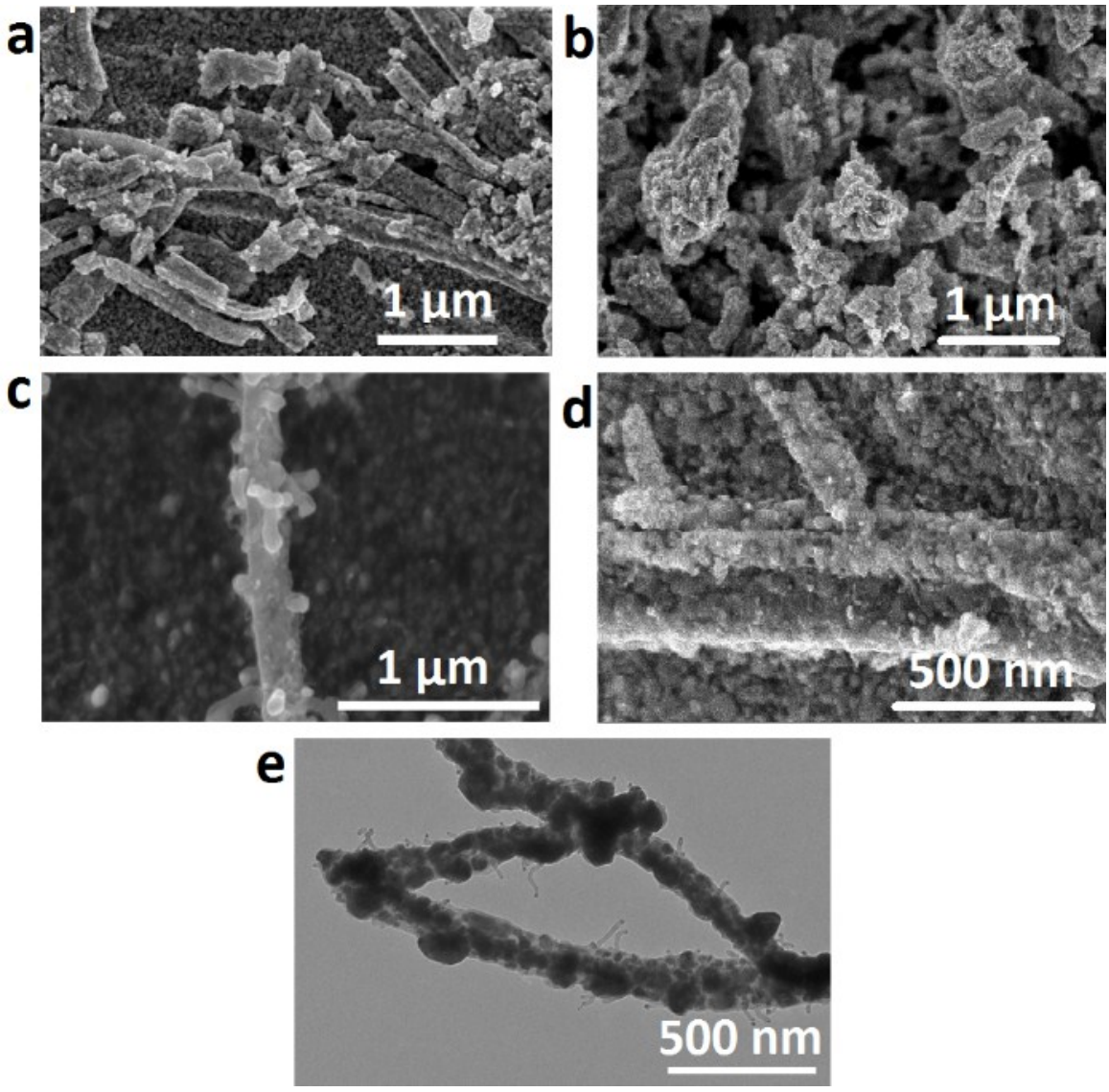

Fig. S8 SEM images of Ni-NF after (a) first cycle and (b) ten cycles, Ni-CNTs-OH after (c) first cycle and (d) ten cycles, (e) TEM image of Ni-CNTs-OH after first cycle.

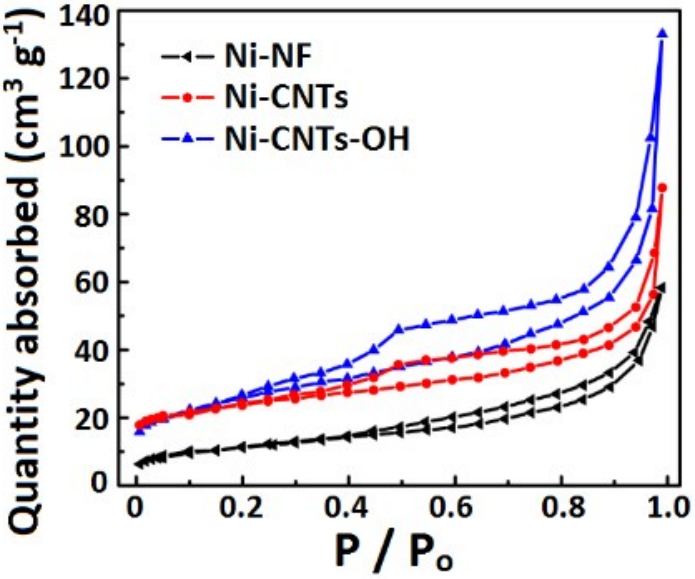

Fig. S9 N_2 adsorption-desorption isotherms of Ni-NF, Ni-CNTs and Ni-CNTs-OH.

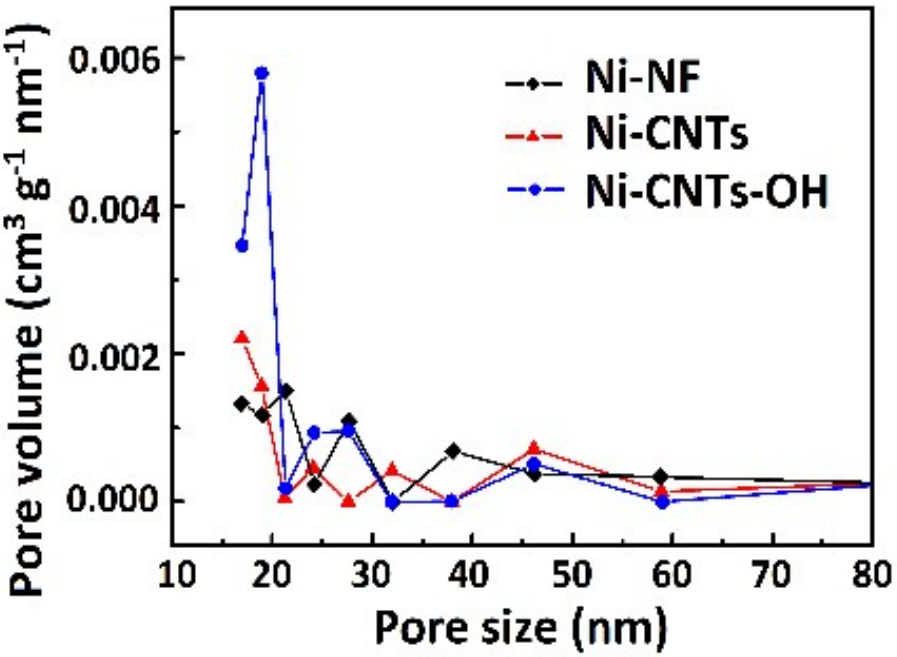

Fig. S10 BJH pore size distributions of Ni-NF, Ni-CNTs and Ni-CNTs-OH.

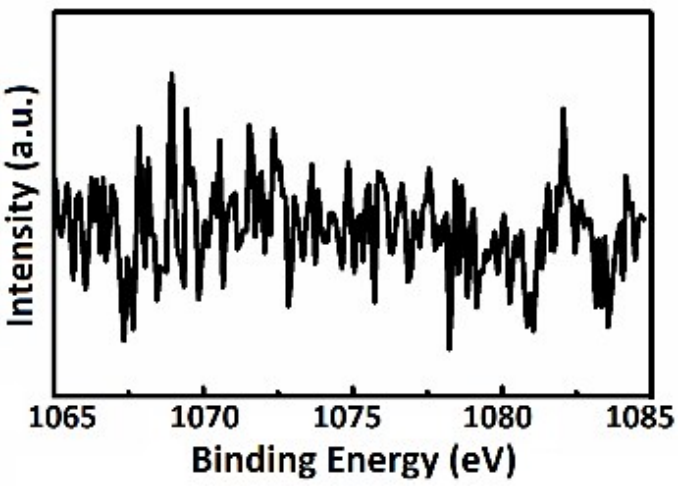

Fig. S11 XPS of Na 1s spectrum of Ni-CNTs-OH after ten cycles of catalytic degradation.